Bond Strength and Failure Mechanisms of Nonconductive Adhesives for Stretchable Electronics

Teemu Salo, Aki Halme, Mikko Kanerva, and Jukka Vanhala, *Member, IEEE*

***Abstract*— Over the past few years, there has been an increasing demand for techniques that allow the forming of stretchable electronics systems from the combination of rigid printed circuit board (PCB) modules and stretchable substrates. The durability issues between the module and interconnects have been solved by optimizing the module's geometry. However, the limiting factor is a reliable attachment method of the module on the substrate. The use of nonconductive adhesives (NCAs) for bonding is one of the most potential techniques due to their low costs and ability to form bonds fast and without a high-temperature cure. In this article, we focused on the testing of different stretchable electronics joints from readily available NCAs and different rigid module materials. The joint samples were tested by using a peel test setup. The fracture surface analysis was carried out by applying the Fourier transform infrared spectroscopy (FTIR). Three different classes of failure mechanisms were identified. The best results were achieved with a novel nonstructural adhesive joint. The nonstructural adhesive joints had a good (0, 28 N/mm) average maximum bond strength with the rigid and smooth FR4 substrate, which made the stretchable substrate elongate considerably (85%) during the peeling. The joint samples from structural adhesives, traditionally used in the electronics industry, were suboptimal.**

***Index Terms*— Adhesive strength, failure analysis, Fourier transform infrared spectroscopy (FTIR), stretchable electronics.**

NOMENCLATURE

ATR	Attenuated total reflection.
CA	Ethylene cyanoacrylate.
FTIR	Fourier transform infrared spectroscopy.
IR	Infrared.
PCB	Printed circuit board.
PLA	Polylactic acid.
PSA	Pressure-sensitive adhesive.
PU	Polyurethane.
NCA	Nonconductive adhesive.
TPU	Thermoplastic polyurethane.

Manuscript received September 16, 2019; revised December 31, 2019 and January 29, 2020; accepted February 15, 2020. Date of publication March 11, 2020; date of current version May 11, 2020. This work was supported in part by the European Union Regional Development Fund (ERDF), Satakunta Regional Council and City of Kankaanpää through the Project A73741 SOFT3L under the Grant 2947/31/2018. Recommended for publication by Associate Editor D. Lu upon evaluation of reviewers' comments. *(Corresponding author: Teemu Salo.)*

Teemu Salo, Aki Halme, and Jukka Vanhala are with the Faculty of Information Technology and Communication Sciences, Tampere University, FI-33014 Tampere, Finland (e-mail: teemu.salo@tuni.fi).

Mikko Kanerva is with the Faculty of Engineering and Natural Sciences, Tampere University, FI-33014 Tampere, Finland.

Color versions of one or more of the figures in this article are available online at http://ieeexplore.ieee.org.

Digital Object Identifier 10.1109/TCPMT.2020.2980121

I. INTRODUCTION

TRADITIONAL electronic circuits are powerful yet inherently rigid. The rigidity restricts the formability and deformation during operation, which further limits the usability of rigid circuits in complex applications. The problem is solved with stretchable electronics that can accommodate very high strains and comply with deformations simply by elongating them [1]. Furthermore, the behavior of the elongation is reliable and provides for compatibility, enabling new implementations of these electronics, such as wearable applications and multisite instrumentation typical of the Internet of Things [2].

Of the many ways to produce stretchable electronics, one way is to attach small intelligent islands on a highly elastic substrate. The islands are, for example, PCBs that hold standard electronic components [2], [3]. The islands are electrically connected by stretchable interconnections on the compliant substrate. The interconnections are shaped and optimized per composition so that they intrinsically elongate until they reach very high maximum strains [4]. The islands form an intelligent network with the interconnections, in which functional operations are distributed to several islands.

The advantage of the island network is that the concept can be implemented with standard manufacturing methods using off-the-shelf components. Well-established manufacturing processes make the stretchable electronics reliable and cost effective to produce [2]. This kind of manufacturing approach is supported by the development of electronics components, which will increase the functional capacity of the islands and decrease their size. The size and shape of islands considerably affect how individual islands interfere with the elongation of the highly compliant substrate. Based on existing work, circular islands—with diameters as high as 18 mm—permit a stretchable system [5].

Stretchable electronics include three types of components: rigid islands, stretchable interconnections, and a highly compliant substrate. Stretchable interconnections have been intensively studied, and 600% elongations have been achieved for interconnections [6], but the connections to a component typically break at 20%–50% [7]. The solutions described previously are difficult to implement when they involve delicate local modification of the substrate or embedded guard structures.

The durability issues between the module and interconnects have been studied extensively [4], [8], [9]. One potential solution is to optimize the module's geometry [4], [10].

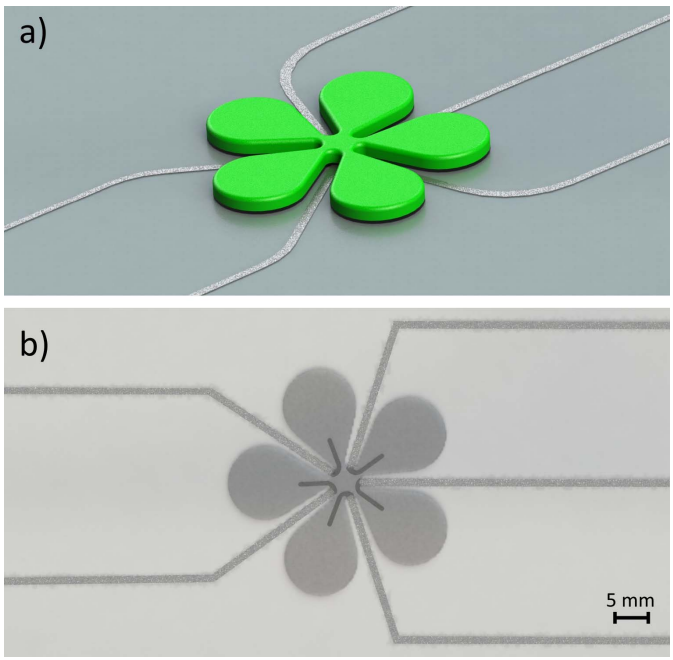

Fig. 1. (a) Proposition for stretchable electronics module design. Clover-shaped module directs deformations away from printed interconnections [10], and compliant (black) PSA tape decreases the stress concentration effect between the module and the substrate. (b) Illustration on how the interconnections turn under the clover-shaped module.

The optimization is based on inwardly curved edges, which form tapered channels through which the interconnections are routed (see Fig. 1). This guides the stress away from the critical area of the component edge and guards the connection between the interconnections and the component.

However, the optimized modules need a proper attachment method to work as stress release. Currently, the limiting factor is the adherence method of the modules on the substrate. In this article, we have investigated the applicability of available adhesives with the materials of stretchable electronics to find the optimal combination for the assembly of the stretchable circuit board.

NCAs have been reported for the use of adhering the components and the islands during the preparation of stretchable conductive joints, focusing on electric properties. The mechanical quality and the durability have received little attention, although long-term durability is a primary challenge in these systems [3]. In this article, the adhesion and the weakest links of various bonds of stretchable electronics joints are studied by means of testing and material characterization. Alternative testing methods and more durable stretchable joint designs are pursued with the cross-disciplinary methods.

II. Theory

A. Methods to Attach Islands on Substrate

When the islands, such as PCBs, and the substrate with the interconnections are joined, they are designed to form electrical and mechanical contacts. The electrical contacts are created between the islands and stretchable interconnections, which form an intelligent stretchable network. The mechanical contacts are made between nonconductive areas of the islands and substrate to protect the electrical contacts from mechanical stresses and corrosion. The islands can be adhered on a substrate with adhesives, mechanical interlocking, or solders.

Adhesives with fillers such as silver flakes and carbon nanotubes are generally versatile and the conductive fillers make the joints conductive. The conductivity depends on the amount and type of the conductive fillers in the adhesive. A high amount of the fillers, i.e., above the percolation threshold, allow isotropic conductivity. A low amount of fillers, i.e., below the percolation threshold, allow anisotropic conductivity (or no conductivity). Both kinds of conductive adhesives, isotropic conductive adhesives and anisotropic conductive adhesives, are used in stretchable electronics. NCA can be added to the conductive adhesive joints; this improves the joints' mechanical strength and decreases the amount of costly conductive adhesive [9].

An alternative option to attach the islands on a highly compliant substrate is the compression joint method, which is especially used in smart textiles. The compression bonds are made by fastening the parts mechanically—that is, by applying pressure to the contacts. The compression joints can be permanent, like rivets [11] or adhesives, or removable, like snap fasteners [12]. When using fasteners, this approach tends to be complicated and expensive to manufacture.

As a third option, solders can be used to create the electrical contacts. Low-temperature solders containing bismuth and/or indium have to be used because of the low thermal softening range of the substrates [13]. NCAs are often used with solders as underfills and later as encapsulators to improve the mechanical strength [3]. However, specialized low-temperature solders are expensive. In addition, reliable contacts to the printed stretchable traces on compliant (and compressive) substrate are difficult to achieve with solders.

NCAs can be used as underfills or as the bonding method to form stretchable electronics joints in all previously described attachment methods. NCAs are used to clamp joints together mechanically and electrically [8], [9], such that the clamping pressure, along with the hardening shrinkage of the NCA, leads to compressive forces at the joint, which maintain the contacts. The formed contacts are also affected by the geometry of the contacts [9]. Using solely NCAs in stretchable electronics is attractive because of the cost-effectiveness and the ability to form bonds fast and at low temperatures. Reduced assembly costs are a result of shorter overall assembly time and adhesives with no additional expensive conductive fillers [8]. However, each attachment method is influenced both by the compatibility between the specific substrates and the NCA and by how the formed joint deforms and fails under stresses. The compatibility depends on various parameters, and this article aims to provide new information about the compatibility of common stretchable electronics substrates and widely used NCAs.

B. Phenomena in the System

The primary requirement for choosing a proper NCA for stretchable electronics is that it needs to fix the surfaces of the

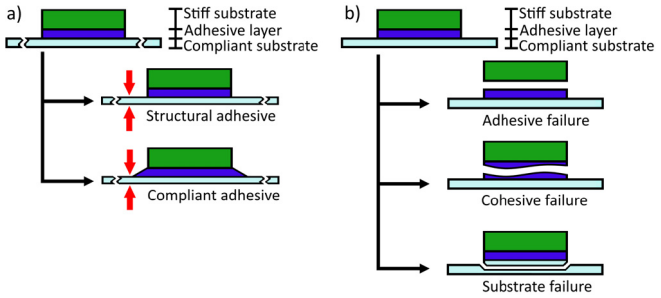

Fig. 2. (a) Behavior of stiff and highly deformable adhesive under uniaxial stretching. (b) Basic failure modes of an adhesive joint.

rigid PCB islands and a highly compliant substrate together. The NCA needs to comply with the deformation differences of materials and, at the same time, maintain adhesion.

Generally, adhesion can be defined as an action when two bodies stick together [14]. In theory, the bond surfaces of the bodies form a common 2-D interface, where adherence of surfaces can be thought to happen. In some cases, depending on the properties of surfaces and expected deformation mechanisms of the joint (e.g., in the stretchable electronics joints), the 2-D interface is better represented by a 3-D interphase. The interphase consists of the interface and the bulk surrounding it, forming the volume for adhesion phenomena, such as mechanical mixing and diffusion, to occur [15].

When NCA is used to attach a PCB island on the substrate, NCA has two different interfaces to adhere to: an interface between the island and the adhesive and an interface between the substrate and the adhesive. The adhesive must wet the surfaces upon preparation to establish interfacial bonds on solid surfaces at the interfaces. Wetting and the flow deformation of an adhesive are affected by the temperature, pressure, and composition [15].

The wetting is also influenced by the properties of the solid surfaces, such as roughness, permeability, and composition. Theoretically, rough surfaces can increase adhesion via a higher surface area, which enables a higher amount of interfacial bonds and mechanical interlocking. However, a too high roughness might lead to voids, which can weaken the joint [15].

Two kinds of NCAs can be used, based on the designed deformation mechanisms in the stretchable electronics joint. The so-called structural adhesives are relatively stiff and can withstand high loads, although the stretchable substrate deforms [16].

Viscoelastic adhesives, such as PSAs, are highly deformable and can follow the substrate under loading [17], [16]. Fig. 2(a) shows the behavior of a structural and a highly deformable adhesive layer.

Adhesives have several parameters that affect the actual bonding strength of the joint. The optimum thickness of the adhesive layer depends on the nature of the adhesive. The cohesive strength of a thick adhesive layer can be less than that of the substrate. Likewise, a variation in the thickness of the adhesive layer offers initiation points for fractures [18]. Furthermore, the exact composition, temperature, humidity, and possible curing agents influence the chemical bond formation within the adhesive [16].

In principle, there are three ways for a joint to fail, which Fig. 2(b) shows. Basically, an adhesive joint can fail in either an adhesive or a cohesive manner. The adhesion failure happens when the adhesive layer does not form sufficient adhesion to bondable surfaces, and the failure occurs cleanly along an interface. The cohesive failure of the adhesive layer happens when the adhesive layer forms a bond stronger than its constitution, and the adhesive layer itself breaks. Moreover, the cohesive failure can occur in the substrate, which causes a type of substrate failure. The substrate failure can occur in the form of substrate delamination or breakage [15], [19].

The strength of the substrate-PCB island system also depends on the local stress–strain gradients [3]. Steep stress–strain gradients typically lead to damage initiation. The failure is caused by a stress concentration effect due to the components having a high mismatch in terms of initial stiffness and stress–strain behavior at high strains [3], [20]. The disadvantageous features of the stress concentration effect can be adjusted by optimizing the islands' shape [10] or by smoothening the deformation differences by gradually stiffening areas around the islands [20], [21]. Additionally, the stress concentration effect can be influenced by the adhesive selection. The selection must also meet the primary requirement of working as a static contact, which might be difficult to achieve using only highly deformable, nonstructural NCAs [8].

C. Modeling as a Part of Designing Interconnections

The testing of various bonding concepts and adhesive products is a laborious activity but is typically necessary up to a certain point. Numerical simulations with validated material models can be used to optimize the geometries of conductive paths (inks), interconnections of PCB modules and the substrates so that electronics in the future could match better deformation of skin and human motion [22], [23]. Valid simulations of strains in the conductive parts of stretchable electronics are the first step on the way to estimate the loading and ultimate failure of adhesive bonds [4]. Furthermore, the modules and possible encapsulation must be accurately modeled [24], [25]. The mode of failure and the properties of the adhesive(s) must be known for the damage of the actual bonding to be properly characterized. The first experiments of the bonding failure can be used as benchmark tests to fit and adjust the numerical models for further optimization routines. Typical methods for these experiments are various tests of adhesion, such as peel tests and pull-off tests. The failure mode observed in a real test provides the knowledge of the damage site, i.e., the model must include a damage model for the specific material or interface that breaks. The behavior of the damage propagation during experimentation can be used to decide whether or not inertia plays a role in the simulation of the test. Finally, a proper combination of tests is needed to fit a 2-D or even a 3-D model with the critical fracture mechanics parameters, such as fracture energy or fracture toughness. Methods on a finite element basis are necessary, especially for the 3-D models.

TABLE I
SUBSTRATE MATERIALS USED IN FOR SAMPLE PREPARATION

Property	Platilon U 4201 AU film	Solder masked FR4 board	3D-printed board
Composition	TPU	Glass fibre reinforced epoxy composite	PLA
Thickness	0.1 mm	1.6 mm	1.8 mm
Nature	Compliant	Stiff	Stiff
Surface	Solid and smooth	Solid and smooth	Permeable and corrugated

TABLE II
SAMPLE TEST SERIES FOR PEEL TESTING

Series	Polymer	Trade name, provider	Time to adhesive achieve handling strength
1	Epoxy	Permabond ET515	0.5 h
2	Epoxy	Permabond MT382	2 h
3	Polyurethane	3M DP610	2 h
4	Cyanoacrylate	Loctite 406	10 s
5	Cyanoacrylate with primer	Loctite 406 with Loctite SF 7239	10 s
6	Pressure-sensitive	3M 8132LE	20 s / 50 °C

III. METHODS

A. Sample Preparation

All of the samples have a 100-μm thick TPU film (Platilon U 4201 AU, by Covestro) representing the highly compliant substrate in the stretchable joint. The length of each film piece is 210 mm (50-mm longer than the "stiff" substrates) so that the film can be fixed to the lower jaw of the tensile test machine. Two kinds of stiff substrates are used: 1) a smooth and solid solder mask-covered (Coates XV501T) green FR4 board; and 2) a rough and permeable 3-D-printed PLA substrate board. The 3-D-printed samples are made with a 0.2-mm layer thickness, and the direction of printing on the surface layer is parallel to the lengthwise direction of the sample. Table I lists the substrates. The bond surfaces of the substrates are cleaned with isopropyl alcohol before applying any of the adhesive candidates.

Table II presents all of the six sample series with the studied adhesive candidates and related times of adhesives to achieve handling strength. We studied four different structural adhesives. Epoxy adhesives are used in the manufacture of traditional electronics and stretchable electronics [21]. Therefore, two kinds of two-component epoxy adhesive systems are used in the specimen preparation: semiflexible toughened ET515 [26] and a modified MT382 for sealing and bonding applications [27], both by Permabond. The other, less conventional structural adhesives for electronics manufacturing are a compliant two-component PU adhesive system Scotch-Weld DP610 (3M) [28] and a one-component CA adhesive system 406 for plastics and elastomeric materials by Loctite [29]. Loctite 406, also Loctite SF 7239 primer that is designed for difficult plastic substrates [30], is used. In total, there are five different structural adhesive candidates.

The samples are prepared by spreading the adhesive (paste) on the substrate pieces and by pressing a substrate piece and TPU film together for a specified time. The duration of the pressing depends on the reported time, which is required for adhesives to acquire sufficient handling strength. The pressing pressure for all the samples is 1.4 kPa. The process was conducted the same way for all the samples in each series to ensure even bond line thickness of parallel samples. In this article, the effect of bond line thickness to adhesion was not studied.

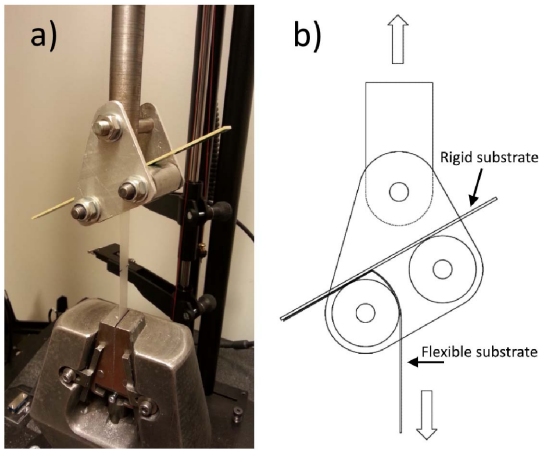

Fig. 3. (a) Floating roller peel test setup with the 45° peel angle used in this article. (b) Schematic diagram of floating roller peel test jig.

As a candidate for compliant adhesives, PSA tape 8132LE (3M) is used. 8132LE tape is 58-μm thick and has support films on both sides prior to bonding [31]. The PSA tape included samples prepared by applying the PSA tape over the substrate pieces, then attaching them on to the TPU film. The adherence of the tape is enhanced by pressing the samples in a press with a 500-kPa pressure for 20 s. The heated plate supporting the sample in the press is heated to 50 °C (the heated plate on the film side).

After all the bonding preparations, all of the six sample series are dried in ambient laboratory conditions for seven days. After the dehydration period and before the peel tests, the specimens are conditioned for 24 h at a temperature of 23 °C and 50% relative humidity (RH).

B. Peel Tests

The behaviors of five NCAs in the assembly of stretchable electronics joints are studied with the floating roller peel test method. The floating roller peel test can be used to determine the bond strength of a sample under a constant peeling speed (50 mm/min) at a 45° peel angle. Here, the peel tests are carried out by using an Instron 5967 tensile test machine with a 2-kN load cell. The floating roller instrument is attached to the movable upper screwhead. Each sample is tested until sample failure or the tensile test machine's limit, which is 300 mm. Fig. 3 shows the peel test setup used.

The value of the momentary adhesion depends on the direction of the peel force, the width of the sample, and the measured force, following the equation below:

$$G_p = F/b(1 - \cos\theta) \tag{1}$$

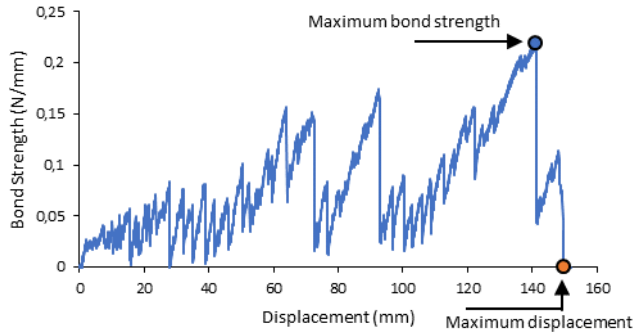

Fig. 4. Typical peel test result and the determined strength values.

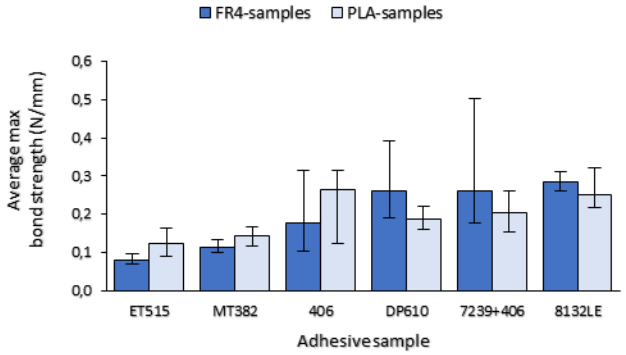

Fig. 5. Average maximum bond strength of the peel test series.

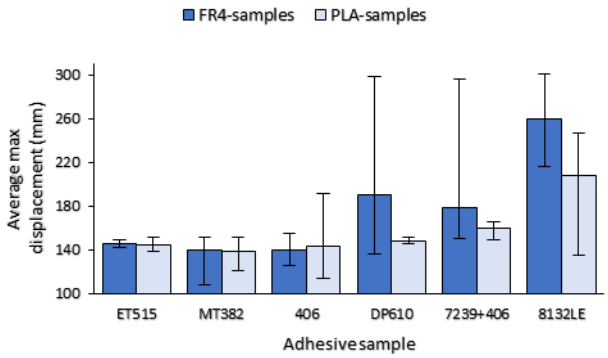

Fig. 6. Average maximum displacement of peel samples.

where G_p is the momentary peel strength (N/mm), F is the measured force (N), b is the width of the sample (mm), and θ is the angle of peel. In this case, the width of the sample is 12 mm and the angle of the peel is 45°. It should be noted that (1) is a simplified form where plastic deformation of the peeled substrate is ignored [32]. In this article, the size of the peel test sample is 160 × 12 mm, in which the peelable length is 140 mm after the gripping and onset of peeling. Six samples per each sample series are tested in order to calculate average and standard deviation values per series.

C. FTIR

By comparing the surfaces of the unused substrates (film and stiff substrates) and the peeled substrates, it is possible to recognize adhesive residues by using a composition-sensitive technique [33].

The peel-tested samples are studied by using a microscope and FTIR device Optics Tensor 27 (Bruker) to determine the microscale quality of the joints and the failure mechanisms at the interfaces. The device has a horizontal ATR unit GladiATR, provided with a diamond crystal. The ATR system used is compatible with the mid-region IR spectrum (4000–400 cm^{-1}) [34]. Background noise is removed by scanning each surface 128 times with a 4-cm^{-1} resolution. The data collected by using the FTIR technique are related to matter at a 1–10-μm depth from the measured surface.

IV. Results

Fig. 4 shows a typical peel test result where the illustrated curve has the indicated maximum (max) bond strength and max displacement values. Additionally, the shapes of the peel test curves are considered with the determined failure mechanisms to conclude with the performance of the NCAs.

A. Determined Bond Strength per Sample Series

Fig. 5 compares the average max bond strengths of the sample series. The highest average max bond strength value is 0.28 N/mm, and the lowest value is 0.08 N/mm. The highest bond strength of 0.28 N/mm is achieved by 8132LE adhesive and the lowest with a value of 0.08 N/mm by ET515—both result with the FR4 substrate. The standard deviations show the result distribution among the six parallel samples, where a low deviation indicates an even debonding process and a high deviation indicates an uneven debonding process.

B. Maximum Displacement During the Peel Tests

The average max displacement recorded until the breakage or test machine limit gives an indication in Fig. 6 of high bond strength (high force required to elongate the TPU film) and stability of the debonding process. Low max displacement indicates poor adhesion. Very high limit strains are desirable for stretchable joints in real products, and the high strains manifest themselves as high displacement in the peel tests. The average max displacement of the tests with the PSA tape and the smooth FR4 substrate is 85% and with the PSA tape and the rough PLA substrate 48% higher than the original peelable length of the samples (140 mm).

Moreover, also with the structural adhesives, the average max displacement in the tests with the PU adhesive DP610 and the FR4 substrate is 38% higher than the peelable length. Likewise, with the primed Loctite 406 and the FR4 substrate, the max displacement is 28% higher than the peelable length.

Figs. 5 and 6 show that peel tests are more complicated when the flexible peel arm is also stretchable. In the sample series, which have high average bond strength, the stretchability of the TPU film (and thus displacement of the tests) is not directly proportional. Typically, when samples have low bond strength, the TPU film does not elongate much. However, each test results in a force-displacement curve, i.e., average or peak values do not resemble all of the behavior. The displacement

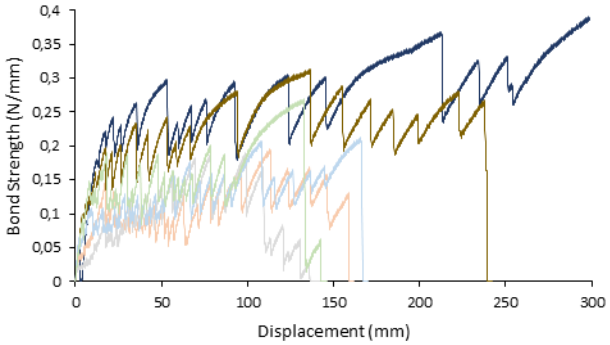

Fig. 7. Peel curves of PU adhesive DP610 with solder masked FR4 substrate. Dark colors indicate samples that had dual interface failure, and light colors represent samples that had adhesive failure on the interface between the adhesive layer and the TPU substrate.

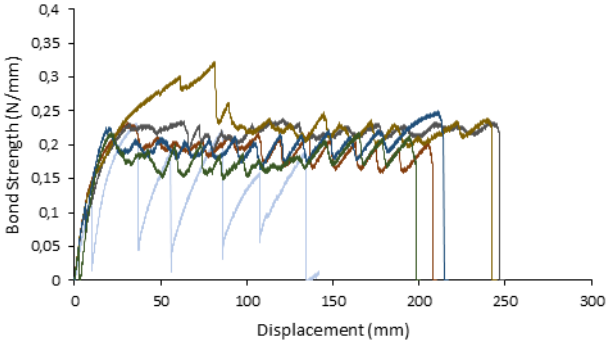

Fig. 8. Peel curves of 8132LE PSA tape with 3-D printed substrate. Dark colors indicate samples, which had adhesive failure on the interface between the tape and the rigid PLA substrate. Light colors represent samples, which had adhesive failure on the interface between the tape and the TPU substrate.

rate is simply a constant (control parameter), but the force is dependent on the dynamic behavior of the nonlinear crack tip-peel arm system.

C. Peel Test Behavior for Structural and Nonstructural Compliant Adhesives

The structural adhesives and the nonstructural, compliant adhesives lead to very different peeling behavior. The peeling occurs in steps with the structural adhesives, which represent stick-slip behavior typical in adhesive joints. Stick-slip behavior indicates development of the plastic crack tip and a subsequent change in the energy dissipation by a shifting of the failure mode. Fig. 7 shows a typical stick-slip behavior in the curves as sudden jumps of values.

In Fig. 7, the samples peel inherently accompanied by random stick-slip behavior. The two samples that have a high average bond strength (over 0.3 N/mm) peel with a failure locus shifting between adhesive substrate and adhesive film interface (determined visually during the tests and later with FTIR-ATR, see Section IV-D). The other four samples with a lower bond strength have simple adhesive failure on the interface between the adhesive layer and the TPU substrate.

The PSA tape including samples generally have a more constant peeling behavior than do the structural adhesive samples. However, the roughness of the 3-D-printed PLA substrate presumably caused regular unevenness and loci of failure initiation, as is seen for most of the sample curves in Fig. 8. An exceptional peeling behavior is observed for one of the samples (8132LE PSA tape), which is explained by a different observed failure mechanism. When the other samples (8132LE PSA tape) mainly have adhesion failure at the interface between the adhesive layer and PLA substrate, the deviate sample has adhesion failure on the interface between the adhesive layer and TPU film.

D. Failure Mechanisms of Peel Samples

Fig. 9 shows typical FTIR results of a substrate (Loctite 406 adhesive-bonded sample). The IR spectrums indicate different absorbance of IR energy, which directly indicates that the chemical compositions of these surfaces differ. Thus, the peeled surface has adhesive residues left after peel testing.

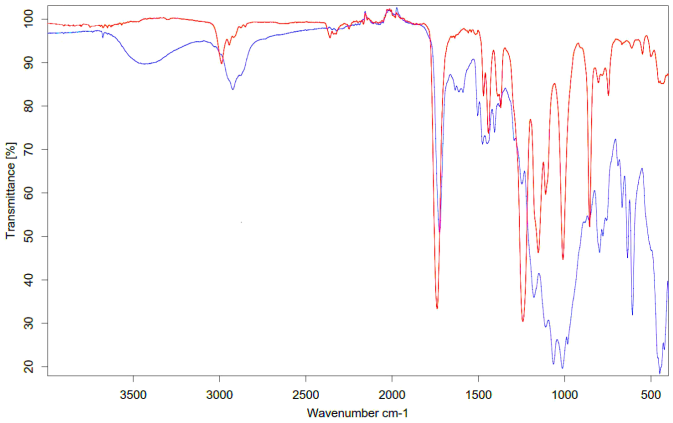

Fig. 9. FTIR-ATR analysis of the reference FR4 substrate (blue) and the FR4 substrate from the Loctite 406 adhesive-bonded sample (red).

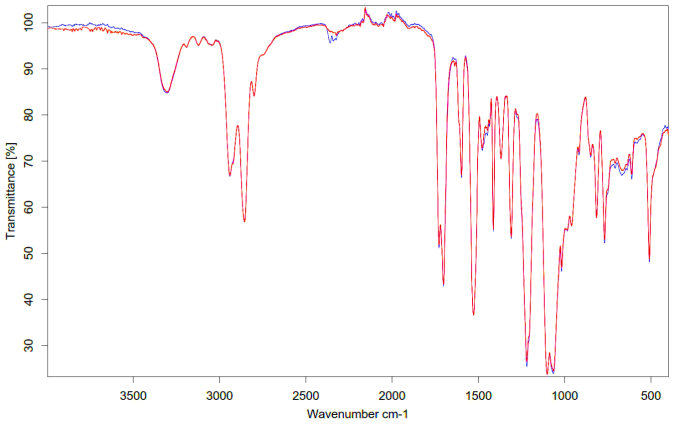

Fig. 10. FTIR-ATR analysis of the reference TPU film (red) and the TPU substrate from the sample DP610 PU adhesive with the FR4 substrate (blue).

The IR spectrums for the samples in this article are either clearly different, representing two different polymers, or identical, as Fig. 10 shows (the variation around 2350 cm^{-1} is caused by moisture and carbon dioxide [35]). Since the "identical" curves also represent the composition of the original surfaces (prior bonding), these samples do not have adhesive residues.

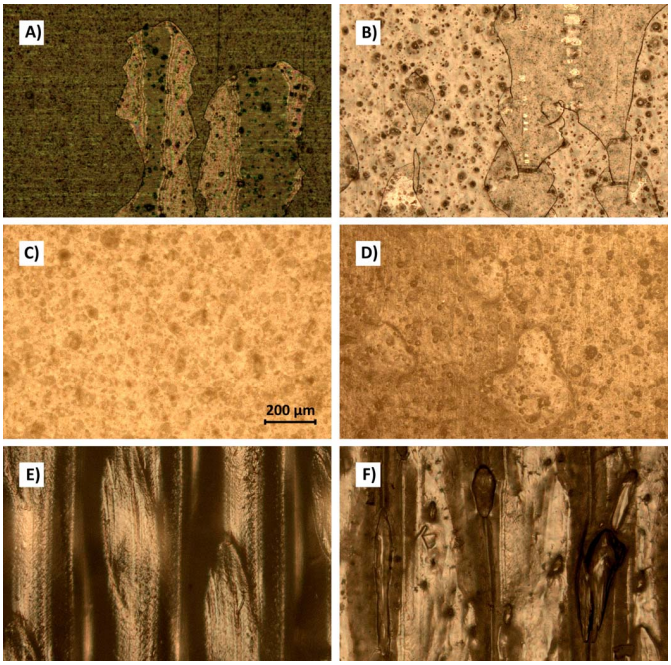

Fig. 11. Microscope images of samples. The peeling direction in the photographs of failed samples is downward. (a) FR4 substrate of the DP610 PU adhesive sample that had dual interface failure. Areas of clean FR4 and the adhesive layer are recognizable. (b) TPU substrate of the same DP610 PU adhesive sample with surfaces of clean TPU substrate and torn adhesive layer. (c) Unpeeled reference TPU substrate. (d) TPU substrate of 406 CA sample that had cohesive failure. Despite the uncolored adhesive, the presence of the adhesive residues can be seen as irregularities on the surface. (e) 3-D-printed PLA substrate of PSA tape sample that had adhesive failure. The tape has peeled cleanly from corrugated 3-D-printed surface. (f) TPU substrate of the same PSA tape sample. The tape on the substrate has deformed and taken the shape of the PLA substrate.

In addition to FTIR, peeled substrates are also studied with microscope imaging and are shown in Fig. 11. Fig. 11(a) and (b) shows the DP610 sample that had a dual interface failure. Fig. 11(c) shows the reference TPU substrate, which visually differs from the TPU substrate of Fig. 11(d), which has irregular adhesive residues on it. Fig. 11(e) introduces a 3-D-printed substrate from a peeled PSA tape sample. The tape has cleanly peeled from the rigid substrate and has remained on the TPU substrate in Fig. 11(f).

The dominant failure mechanism per sample series can be identified and established after visual inspection, microscope examination, and FTIR inspections. The results are categorized into three failure mode groups, which are presented in Table III.

From the observed failure modes, the epoxy adhesive-bonded and PU adhesive-bonded samples tend to have the adhesive failure on a single interface between the adhesive layer and the TPU substrate when the FR4 substrate is used. For the samples with the rough PLA substrate, adhesion failure occurred in a random manner at both interfaces of the adhesive layer.

The second failure mode pattern can be seen for the Loctite 406 CA adhesive-bonded samples with or without the primer Loctite SF 7239. Failure occurs as a cohesive failure in the adhesive layer in all the four series, despite the determined high standard deviation in the series results (of peel strength).

TABLE III
DOMINANT FAILURE MODES OF PEEL TEST SAMPLES

Adhesive	Substrate	Dominant failure mechanism	Failure type
ET515 epoxy	Solder masked FR4		I
ET515 epoxy	3D-printed PLA		
MT382 epoxy	Solder masked FR4		
MT382 epoxy	3D-printed PLA		
DP610 PU	Solder masked FR4		
DP610 PU	3D-printed PLA		
Loctite 406 CA	Solder masked FR4		II
Loctite 406 CA	3D-printed PLA		
primed Loctite 406 CA	Solder masked FR4		
primed Loctite 406 CA	3D-printed PLA		
8132LE PSA tape	Solder masked FR4		III
8132LE PSA tape	3D-printed PLA		

For all the test series, TPU film is peeled from the substrate.

The sample series with the PSA tape stand out from the structural adhesive series and lead to mainly adhesive failure at the interface between the tape and the stiff substrates that are typically deemed as unacceptable in adhesive joints. While the compliant adhesive totally remains on the TPU substrate, the strength values represented promising results. The PSA tape samples have high resistance against peeling, high bond strength, and steady debond process. The PSA tape on the fracture surface actually remains sticky after the peel testing, and it has an ability to reattach back to the surfaces.

V. DISCUSSION

The peel tests were successfully performed and carefully analyzed to understand the behavior and bond quality of different film–substrate combinations. A high elongation of the TPU film-substrate increases the elastic energy stored in the test setup during the testing. Since the TPU film primarily deforms in an elastic manner, the peel strength values are essentially anticipated correctly. However, any plastic dissipation in the film could be subtracted to provide more accurate fracture energy values, for example, for modeling purposes [32], [33]. The elasticity of the peel arm (film) is seen in Fig. 7 from the recorded peel curves. It can be assumed that the first linear increase in the curves is caused by the reversible elastic deformations in the TPU substrate [33], which changes to less steep because the elastic deformations change to irreversible plastic deformation [36].

The properties of the adhesive layers, i.e., thickness, area, and geometry, influence the load distribution in real application joints. The floating roller peel tests are clearly more demanding for the stretchable joints than their actual applications because the crack tip stresses are induced in a single planar direction. Furthermore, the TPU substrate in wearable

applications is usually laminated on a textile or other substrate, which stiffens the stretchable joint and may also increase its durability. It should be noted that there are different approaches for peel testing [32], [33]. Here, the standard preparing conditions of the samples were applied to ensure comparable results from all the sample series, but the air humidity could have affected the adhesives differently [16]—the results are specific to the selected test condition (50% RH).

A. Analysis of Failure Type I Samples

The dominant failure mode of the epoxy adhesive and the PU adhesive samples with the solder masked FR4 substrates is adhesion failure at the interface between the adhesive layer and the TPU substrate. In turn, the failure of the samples with the 3-D-printed PLA substrates is the randomly located adhesive failure on both interfaces of the adhesive layer.

The epoxy adhesives formed poor adhesion on the TPU substrate and are not a good choice for stretchable electronics joints. Between the samples, the PLA substrate samples have a slightly higher average bond strength than the FR4 substrate samples, which is explained by the failure mechanisms. The epoxy adhesive samples have the same degree of adhesion when the adhesion failure occurred along a single interface that increased when the adhesive layer was torn and the failure occurred simultaneously at both interfaces. Tearing of the adhesive layer was the phenomenon that consumed additional energy and was caused by the thickness variations of the adhesive layer.

The PU adhesive-bonded samples have a higher average bond strength than the epoxy adhesive-bonded samples, which is caused by a higher amount of adhesion between the adhesive and the TPU substrate. There were also challenges in the preparation of the PU adhesive DP610, including samples. The adhesive required seven days in total to fully dry after the manufacturer-specified time to achieve handling strength [28]. The adhesive is also sensitive to moisture [16], which causes bubbles inside the adhesive layer during curing.

B. Analysis of Failure Type II Samples

As seen in Table III, cohesive failure is the dominant failure mode of the CA adhesive-bonded samples. The conclusion is confirmed by the FTIR analysis on a microscale. Generally, cyanoacrylates cure rapidly at room temperature [16], [29]. Despite the time window of CA adhesive to achieve handling strength, the cure of the CA adhesive might have already begun before the clamping, which increases any variations in the quality of the adhesive layer. Additionally, the primer can work as an activator and accelerate the CA curing [30]. The surface topography of the stiff substrates also causes variations to the local microscale thickness of the adhesive layer. A thin adhesive layer is generally considered durable with cyanoacrylates [37].

The fast curing reaction of the CA adhesive is a disadvantage for manual bonding but can be an advantage for industrial mass production. The results indicate that the CA adhesive adheres very well on both TPU film and the stiff substrates. The adhesive could be used in the stretchable electronics joints, especially when the adhesive layer's thickness is optimized.

C. Analysis of Failure Type III Samples

The results of the samples with PSA tape stand out when comparing the structural adhesives and the failure modes. The mechanical properties of the PSA tape are closer to the properties of the TPU film than the other tested adhesives. The dominant failure mode occurs in the form of adhesive failure at the interface between the adhesive layer and the stiff substrate. However, these samples have satisfactory average bond strength values with a low standard deviation and high max displacements.

The failure mechanism allowed regular peeling of the TPU film from the PSA tape-treated samples because the PSA tape elongates rather equally with the TPU film. The challenge, in reality, with this type of result is that the peel test performance with a very high elongation does not represent well the biaxial (or even tri-axial) loadings amid real PCBs. For a real planar design, the PCB surroundings must be redesigned to allow for enhanced compliance, imitating the free edges of the slender specimens in the peel test. Fig. 1(a) shows a proposition for stretchable electronics modules design to improve the applicability and full potential of the excellent peel test results. The design uses clover-shaped PCBs, which decrease deformations of printed interconnections [10], and compliant PSA tape, which decreases the mismatch between the rigid PCB and the highly compliant substrate.

In real applications, the PSA tape can reattach after failure but cannot alone support high-quality electrical connections in the stretchable electronics joint (after bond failure). The clover-shaped module allows the contacts to be routed to each "leaf" like arm, shown in Fig. 1(b), where the PSA tape does not elongate as much at the module's edges. Moreover, compliant adhesive joints could be gradually stiffened by using the same stiffening methods that are used currently in the stretchable electronics [1], [20], [38].

VI. Conclusion

Conventional NCAs, when used in the manufacturing of rigid electronics, are not suitable as durable adhesives in stretchable electronics. NCAs are still an attractive attachment method for the stretchable electronics because of their cost-effectiveness and simplicity. In this article, the debond onset and the process of different NCAs are studied with six different adhesive test series and two different rigid-type substrates.

The results emphasize the completely different bond formation by structural adhesives and the more compliant "elastic" adhesives in the stretchable joints. The epoxy and PU structural adhesives lead to stick-slip behavior and mixed-mode failure at the glue line. An optimal level of dual interfacial failure gives the highest bond strength values for these adhesives. Moreover, the CA structural adhesives induced cohesive failure in the glue line despite highly varying bond strength values during the tests. The bond strength could be increased and made more consistent for these systems by optimizing the thickness and processing of the adhesive layer.

In contrast to the structural adhesives that resemble more rigid substrates after curing, the compliant adhesive PSA tape behaves (from the mechanical point of view) like the TPU film in the peel tests. The compatibility with the TPU film enhanced the bond strength and allowed the optimal failure process for stretchable joints. The main failure mechanism type of these samples was adhesive failure, yet the peel strength and displacement of the compliant adhesive series were among the best of the total test series.

The compliant adhesive joints, with different levels of target deformability, could be used to increase the elongation of a stretchable electronics structure. PSA tape-type adhesives can be used to bond rigid islands with clover-shaped modules to apply the full potential of highly compliant interfaces and the results by standard peel testing. Clearly, the overall planar shaping of PCB joints is needed to increase the durability of joints with extensive deformations.

ACKNOWLEDGMENT

The authors would like to thank researchers O. Orell and S. Siljander for their assistance with the testing activities.

REFERENCES

[1] N. Matsuhisa *et al.*, "Printable elastic conductors with a high conductivity for electronic textile applications," *Nature Commun.*, vol. 6, no. 1, Nov. 2015, Art. no. 7461.

[2] F. Bossuyt, T. Vervust, and J. Vanfleteren, "Stretchable electronics technology for large area applications: Fabrication and mechanical characterization," *IEEE Trans. Compon., Packag., Manuf. Technol.*, vol. 3, no. 2, pp. 229–235, Feb. 2013.

[3] T. Someya, Ed., *Stretchable Electronics*. Weinheim, Germany: Wiley, 2012, p. 462.

[4] M. Mosallaei *et al.*, "Geometry analysis in screen-printed stretchable interconnects," *IEEE Trans. Compon., Packag., Manuf. Technol.*, vol. 8, no. 8, pp. 1344–1352, Aug. 2018.

[5] R. Vieroth *et al.*, "Stretchable circuit board technology and application," in *Proc. Int. Symp. Wearable Comput.*, Linz, Austria, Sep. 2009, pp. 33–36.

[6] T. Araki, M. Nogi, K. Suganuma, M. Kogure, and O. Kirihara, "Printable and stretchable conductive wirings comprising silver flakes and elastomers," *IEEE Electron Device Lett.*, vol. 32, no. 10, pp. 1424–1426, Oct. 2011.

[7] A. Jahanshahi, P. Salvo, and J. Vanfleteren, "Stretchable biocompatible electronics by embedding electrical circuitry in biocompatible elastomers," in *Proc. Annu. Int. Conf. IEEE Eng. Med. Biol. Soc.*, San Diego, CA, USA, Aug. 2012, pp. 6007–6010.

[8] P. Foerster, C. Dils, C. Kallmayer, T. Loher, and K.-D. Lang, "First approach to cost-efficient fine pitch NCA flip-chip assembly on thermoplastic polyurethane printed circuit boards," in *Proc. 4th Electron. Syst.-Integr. Technol. Conf.*, Amsterdam, The Netherlands, Sep. 2012, p. 6.

[9] C. Goth, "Connection mediums," in *Three-Dimensional Molded Interconnect Devices (3D-MID)*, J. Franke, Ed. Munich, Germany: Carl Hanser Verlag GmbH & Company KG, 2014, pp. 143–148.

[10] P. Iso-Ketola, J. Vanhala, and M. Mäntysalo, "Extensible construction comprising a conductive path and method of manufacturing the structure," Google Patent FI 127 173 B, Dec. 29, 2017.

[11] W. A. Hufenbach, F. Adam, T. Möbius, D. Weck, and A. Winkler, "Experimental investigation of combined electrical and mechanical joints for thermoplastic composites," in *Proc. Tech. Conf. Exhib. (ANTEC)*, Las Vegas, NV, USA, Apr. 2014, pp. 592–595.

[12] A. Mehmann, M. Varga, and G. Tröster, "Reversible contacting for smart textiles," in *Smart Textiles*, S. Schneegass and O. Amft, Eds. Cham, Switzerland: Springer, 2017, pp. 185–198.

[13] E. E. M. Noor, H. Zuhailawati, and O. J. Radzali, "Low temperature In-Bi-Zn solder alloy on copper substrate," *J. Mater. Sci., Mater. Electron.*, vol. 27, no. 2, pp. 1408–1415, Feb. 2016.

[14] R. J. Good, "Semantic physics of adhesion," in *Treatise on Adhesion and Adhesives*, vol. 5, R. L. Patrick, Ed. New York, NY, USA: Marcel Dekker, 1981, p. 295.

[15] F. M. da Silva, A. Öchsner, and R. D. Adams, Eds., *Handbook of Adhesion Technology*. Berlin, Germany: Springer, 2011, p. 1554.

[16] F. C. Campbell, "Adhesive bonding," in *Joining—Understanding the Basics*, F. C. Campbell, Ed. Ohio, OH, USA: ASM International, 2011, pp. 243–277.

[17] M. M. Feldstein, E. E. Dormidontova, and A. R. Khokhlov, "Pressure sensitive adhesives based on interpolymer complexes," *Progr. Polym. Sci.*, vol. 42, pp. 79–153, Mar. 2015.

[18] D. A. Dillard, "Stress distribution: Bond thickness," in *Handbook of Adhesion*, D. E. Packham, Ed., 2nd ed. Chichester, U.K.: Wiley, 2005, pp. 494–496.

[19] *Adhesives. Designation of Main Failure Patterns*, document SFS-10365, Finnish Standards Association, Helsinki, Finland, 1995.

[20] I. M. Graz, D. P. J. Cotton, A. Robinson, and S. P. Lacour, "Silicone substrate with *in situ* strain relief for stretchable thin-film transistors," *Appl. Phys. Lett.*, vol. 98, no. 12, Mar. 2011, Art. no. 124101.

[21] I. Chtioui, F. Bossuyt, and M. H. Bedoui, "Thermo-plastically stretchable electronic and sensor circuits," in *Proc. 17th Int. Conf. Electron. Packag. Technol. (ICEPT)*, Wuhan, China, Aug. 2016, pp. 1396–1400.

[22] H. Joodaki and M. B. Panzer, "Skin mechanical properties and modeling: A review," *Proc. Inst. Mech. Eng., H, J. Eng. Med.*, vol. 232, no. 4, pp. 323–343, Apr. 2018.

[23] J. M. Benítez and F. J. Montáns, "The mechanical behavior of skin: Structures and models for the finite element analysis," *Comput. Struct.*, vol. 190, pp. 75–107, Oct. 2017.

[24] M. Mosallaei, J. Jokinen, M. Kanerva, and M. Mäntysalo, "The effect of encapsulation geometry on the performance of stretchable interconnects," *Micromachines*, vol. 9, no. 12, p. 645, Dec. 2018.

[25] H. Varner, J. Mahaffey, T. Marinis, and C. DiBiasio, "Encapsulation of microelectronic assemblies for use in harsh environments," in *Proc. Int. Symp. Microelectron.*, no. 1, Oct. 2017, Art. no. 000292.

[26] *Permabond ET515 Technical Datasheet*, Permabond LLC, Pottstown, PA, USA, Oct. 2016.

[27] *Permabond MT382 Technical Datasheet*, Permabond LLC, Pottstown, PA, USA, Feb. 2018.

[28] *Scotch-Weld EPX Clear Adhesive DP610 Product Data Sheet*, Suomen 3M Oy, Espoo, Finland, 2011.

[29] *Loctite 406 Technical Data Sheet*, Henkel, Düsseldorf, Germany, Feb. 2012.

[30] *Loctite SF 7239 Technical Data Sheet*, Henkel, Düsseldorf, Germany, Oct. 2015.

[31] *3M Adhesive Transfer Tape 8132LE*, 3M, Saint Paul, MN, USA, 2019.

[32] B. A. Morris, "Fracture mechanics analysis of peel test," in *Science and Technology of Flexible Packaging*, B. A. Morris, Ed. Oxford, U.K: William Andrew, 2017, pp. 354–360.

[33] M. Nase, B. Langer, and W. Grellmann, "Fracture mechanics on polyethylene/polybutene-1 peel films," *Polym. Test.*, vol. 27, no. 8, pp. 1017–1025, Dec. 2008.

[34] J. S. Gaffney, N. A. Marley, and D. E. Jones, "Fourier transform infrared (FTIR) spectroscopy," in *Characterization of Materials*, E. N. Kaufmann, Ed., 2nd ed. New York, NY, USA: Wiley, 2012, pp. 1104–1135.

[35] J. M. Chalmers, "Mid-infrared spectroscopy: Anomalies, artifacts and common errors," in *Handbook of Vibrational Spectroscopy*, J. M. Chalmers and P. R. Griffiths, Eds. Hoboken, NJ, USA: Wiley, 2006, pp. 2327–2347.

[36] A. J. Kinloch and J. G. Williams, "The mechanics of peel tests," in *Adhesion Science and Engineering*, vol. 1, D. A. Dillard, A. V. Pocius, and M. Chaudhury, Eds. Amsterdam, The Netherlands: Elsevier, 2002, pp. 273–301.

[37] B. Goss, "Cyanoacrylates," in *Practical Guide to Adhesive Bonding of Small Engineering Plastic and Rubber Parts*, B. Goss, Ed. Shawbury, U.K.: ISmithers, 2010, pp. 1–8.

[38] N. Karyu, M. Noda, S. Fujii, Y. Nakamura, and Y. Urahama, "Effect of adhesive thickness on the wettability and deformability of polyacrylic pressure-sensitive adhesives during probe tack test," *J. Appl. Polym. Sci.*, vol. 133, no. 27, p. 11, Jul. 2016.